Journal of Statistical Physics, Vol. 69, Nos. 1/2, 1992

A Multineuron Interaction Model for Neural Networks

J. J. Arenzon,[1] R. M. C. de Almeida,[1] and J. R. Iglesias[1]

Received February 25, 1992

A multineuron interaction model (RS model) with an energy function given by the product of the squared distances in phase space between the state of the net and the stored patterns is studied in detail within a mean-field approach. Two limits are considered: when the patterns and antipatterns are stored (as in the Hopfield model), PAS case, and when only the patterns are taken into account, OPS case. The $T=0$ solutions for the proper memories are exactly obtained for all finite values of α, as a consequence of the energy function: whenever one of the overlaps is exactly one the corresponding equations decouple and no configuration average is required. Special interest is focused on the OPS situation, which presents a peculiar phase space topology. On the other hand, the PAS configuration recovers the Hopfield model in the appropriate limit, while keeping associative memory abilities far beyond the critical values of other models when the full Hamiltonian is considered.

KEY WORDS: Neural networks; multineuron interaction.

1. INTRODUCTION

Connected arrays of binary spins are one possible way to idealize neural systems[1,2] and the main objectives of such systems are (i) to understand storage, retrieval, and processing of information in the brain and hence other complex functions such as creation, intelligence, logical manipulation, etc.; and (ii) the design of computers capable of executing these complex functions.

The determinant characteristic of human memory is to be content-addressable, i.e., the necessary stimulus required to retrieve a pattern is a portion of its information, in contrast to the physical bit address of a variable in an ordinary computer. The brain, where the information is

[1] Instituto de Física, Universidade Federal do Rio Grande do Sul, 91540 Porto Alegre, RS, Brazil.

0022-4715/92/1000-0385$06.50/0

stored, is composed of neurons that may or not emit electric signals through their axons to the dendrites of other neurons.[3] Both axons and dendrites may extend to macroscopic scales and, depending on the region of the brain in which the neurons are located, they are so richly branched that the network resembles an entanglement of filaments. A way to model such an associative memory system is to consider a network of infinite-range interacting binary spins ($S_i = \pm 1$) that are associated with the state of the neurons (active or inactive).[1,2] A given prescription of an energy function that describes the neuron interactions, and the way it changes when a new pattern is learnt, defines one possible model for associative memory with a performance that can be measured through the storage capacity of the net and its ability to recognize similar but not equal patterns.

The phase space of a network with N spins is the set of all vertices of an N-dimensional hypercube, and a possible configuration of the net is represented by an N-dimensional vector $\mathbf{S}$, given by

$$\mathbf{S} = (S_1, S_2, \ldots, S_N); \qquad S_i = \pm 1 \tag{1}$$

where S_i is the state of the ith neuron. Each amount of information (a pattern) to be learnt by the net is associated with a given configuration of the system. Then, if P of these configurations are chosen, they can be represented by P N-dimensional vectors ξ^μ:

$$\xi^\mu = (\xi_1^\mu, \xi_2^\mu, \ldots, \xi_N^\mu) \tag{2}$$

where $\xi_i^\mu = \pm 1$ and $\mu = 1, \ldots, P$.

The load parameter α is defined as

$$\alpha = \frac{P}{N} \tag{3}$$

and the critical load parameter α_c is the maximum value of α for which the net keeps its associative memory abilities. The degree of similarity between two states of the system, say $\mathbf{S}^{(1)}$ and $\mathbf{S}^{(2)}$, is related to the number of aligned neurons and can be measured by the overlap m, defined as

$$m = \frac{1}{N} \sum_{i=1}^{N} S_i^{(1)} S_i^{(2)} \tag{4}$$

Then, if $\mathbf{S}^{(1)} = \mathbf{S}^{(2)}$, $m = 1$; if $\mathbf{S}^{(1)} = -\mathbf{S}^{(2)}$, $m = -1$; and if $\mathbf{S}^{(1)}$ and $\mathbf{S}^{(2)}$ are uncorrelated, $m \approx 0$ (of order of $1/\sqrt{N}$). The overlap m_μ of an arbitrary initial state $\mathbf{S}(t=0)$ with the μth stored pattern is

$$m_\mu(0) = \frac{1}{N} \sum_{i=1}^{N} \xi_i^\mu S_i(0) \tag{5}$$

and the net works as an associative memory if its dynamics (to be defined later) is such that, starting from a given, finite value of m_μ, the evolution leads to a stable state $m_\mu \approx 1$. This clearly means that $\mathbf{S} = \xi^\mu$ are minima of the energy function $E(\mathbf{S})$ that describes the interactions between the neurons. Then a possible definition of the critical load parameter α_c is the maximum value of α for which the patterns are still minima of $E(\mathbf{S})$.[4,5] The best known model for neural networks is the Hopfield model.[2–4] It considers an array of N binary spins (neurons), coupled through synaptic connections J_{ij}, described by an Ising Hamiltonian:

$$H = -\frac{1}{2} \sum_{i=1}^{N} \sum_{j \neq i}^{N} J_{ij} S_i S_j \tag{6}$$

As the memorized patterns should be minima of H, and they are determined by the values of J_{ij}, the learning process of new memories is described through convenient modifications of the synaptic connections prescribed by learning rules; in the original Hopfield model the synaptic connections are given by the generalized Hebb learning rule[2–4,6]:

$$J_{ij} = \frac{1}{N} \sum_{\mu=1}^{P} \xi_i^\mu \xi_j^\mu \tag{7}$$

and they describe satisfactorily an associative memory dynamics provided that the net is not overcrowded, i.e., $\alpha < \alpha_c \approx 0.14$[4] and the learnt patterns are not correlated,[4,7] that is, the overlap between any two memories is of the order of $1/\sqrt{N}$. When $\alpha > \alpha_c$ and/or the patterns are correlated the retrieving abilities of the net are seriously affected: it forgets the learnt patterns ($\alpha > \alpha_c$) or it mixes up similar (correlated) stored patterns. Also, spurious states, i.e., minima not learnt, appear together with the stored patterns.

Some attempts to bypass these and other less important difficulties of the Hopfield model have been made by introducing different learning rules[4,5,8,9] or different energy functions,[10,11] but the results are not remarkably efficient. In this paper we present in full detail a different prescription, which we call the RS model, that has been recently introduced.[12,13] It considers multineuron interactions and has as its origin a very simple idea: the energy of a given configuration is proportional to the squared Euclidean distances in phase space between the state of the net and the stored patterns. The idea of multispin interaction is not new and several works in this direction have been published. For example, Gardner[10] proposed a Hamiltonian that is a generalization of the Hopfield model and Hebb learning rule considering a monomial of degree $p > 2$ in the Ising

spins: Horn and Usher[14] introduced different weights in the p-monomial Hamiltonian to differentiate the several memorized patterns and Abbott and Arian[15] considered, instead, polynomials of degree p in the Ising spins. In spite of the fact that the consideration of multineuron interactions is not original, the way we introduce this feature here is new and the model improves qualitatively and quantitatively previous results. Also, in the Hopfield model, the energy of a given state $\mathbf{S}$ and of its antipode $-\mathbf{S}$ is the same: whenever a pattern ξ^μ is a minimum of H, it is the "antipattern" $-\xi^\mu$. This is not the case of the RS model. Nevertheless, it is always possible to explicitly "teach" the net both patterns ξ^μ and $-\xi^\mu$. This case was preliminary discussed in ref. 12. Actually, the two extreme cases, when *p*atterns and *a*ntipatterns are *s*tored (PAS) or when *o*nly the *p*atterns are *s*tored (OPS), present strikingly different behaviors and we shall discuss them separately.

In the two following sections we present the model and mean-field calculations, and in Section 4 we discuss the results and conclude.

2. THE RS MODEL

The Hamiltonian for a net of N spins is[12,13]

$$H = N \prod_{\mu=1}^{P} \left[\frac{1}{2N} \sum_{i_\mu=1}^{N} (\xi_{i_\mu}^\mu - S_{i_\mu})^2 \right] \tag{8}$$

where P is the number of stored patterns $\xi^\mu = (\xi_1^\mu, \ldots, \xi_N^\mu)$ for $\mu = 1, \ldots, P$, and $\mathbf{S} = (S_1, \ldots, S_N)$ is the state of the net, as before. The μth sum over the spins is the squared Euclidean distance in phase space between the state of the net $\mathbf{S}$ and the μth pattern. From Eq. (8) it is clear that $H(\mathbf{S}) \geqslant 0$ and $H(\mathbf{S}) = 0$ if $\mathbf{S} = \xi^\mu$, for any $1 \leqslant \mu \leqslant P$. This means that, no matter how many patterns are stored (how large α is), the patterns are always minima of H. This suggests that the load limit for this model can be greatly enhanced, in agreement with recent numerical simulations.[16,17] Another interesting feature is that the height of the energy barriers between two patterns depends on the distances between them in the phase space, implying that the barriers are lower when the patterns are nearer each other in phase space, i.e., when they are similar.

The multineuron interaction feature of Eq. (8) becomes evident when it is written as

$$H = N \left(1 + \sum_{i_1=1}^{N} J_{i_1}^1 S_{i_1} + \sum_{i_1, i_2}^{N} J_{i_1 i_2}^2 S_{i_1} S_{i_2} + \cdots + \sum_{i_1, \ldots, i_P}^{N} J_{i_1 \cdots i_P}^P S_{i_1} S_{i_2} \cdots S_{i_P} \right) \tag{9}$$

where

$$J^K_{i_1 \cdots i_K} = \frac{(-1)^K}{N^K} \sum_{\mu_1 < \cdots < \mu_K} \xi^{\mu_1}_{i_1} \xi^{\mu_2}_{i_2} \cdots \xi^{\mu_K}_{i_K} \tag{10}$$

The synaptic connections $J^K_{i_1 \cdots i_K}$ are clearly the strengths of the interactions between K-adics of neurons, and their laws of formation, Eqs. (10), are the equivalent to the Hebb learning rule. Explicitly, the modification in the connections when a new pattern is learned can be achieved by the following algorithm:

$$\begin{aligned} J^{P+1}_{i_1 \cdots i_{P+1}} &= J^P_{i_1 \cdots i_P} \xi^{P+1}_{i_{P+1}} \\ J^P_{i_1 \cdots i_P} &= J^P_{i_1 \cdots i_P} + J^{P-1}_{i_1 \cdots i_{P-1}} \xi^{P+1}_{i_P} \\ &\vdots \qquad\qquad \vdots \\ J^1_{i_1} &= J^1_{i_1} + \xi^{P+1}_{i_1} \end{aligned} \tag{11}$$

and must follow the above order: first J^{P+1} and last J^1. When both patterns and antipatterns are considered, the odd-K synaptic connections are zero and Eqs. (9) and (10) reduce to

$$H = N\left(1 + \sum_{i_1, i_2}^{N} J^2_{i_1 i_2} S_{i_1} S_{i_2} + \cdots + \sum_{i_1, \ldots, i_{2P}}^{N} J^{2P}_{i_1 \cdots i_{2P}} S_{i_1} S_{i_2} \cdots S_{i_{2P}}\right) \tag{12}$$

with

$$J^K_{i_1 \cdots i_K} = \frac{(-1)^{K/2}}{N^K} \sum_{\mu_1 < \cdots < \mu_{K/2}} \xi^{\mu_1}_{i_1} \xi^{\mu_1}_{i_2} \cdots \xi^{\mu_{K/2}}_{i_{K-1}} \xi^{\mu_{K/2}}_{i_K} \tag{13}$$

for a net storing P patterns and the corresponding P antipatterns. The differences between Eqs. (9)–(10) and (12)–(13) reflect the diverse behaviors of the PAS and OPS configurations. For both cases, when only uncorrelated memories are considered, the average of the strengths of interactions is zero for all K orders and the dispersion around zero gives a first estimate of their relevance in the dynamics of the net. Equations (10) and (13) reduce to sums of random walk steps and the ratio of the dispersions ΔJ^K is

$$\frac{\Delta J^K}{\Delta J^{K-1}} = \frac{1}{N}\left(\frac{P - K + 1}{K}\right)^{1/2} \leqslant \left(\frac{\alpha}{N}\right)^{1/2} \tag{14}$$

for the OPS case, and

$$\frac{\Delta J^K}{\Delta J^{K-2}} = \frac{1}{N^2}\left(\frac{P - K/2 + 1}{K/2}\right)^{1/2} \leqslant \left(\frac{\alpha}{N^3}\right)^{1/2} \tag{15}$$

for the PAS configuration. In Eq. (15) we consider P patterns and P antipatterns.

Both ratios, Eqs. (14) and (15), goes to zero for finite $\alpha = P/N$ and $N \to \infty$, i.e., as the order of the synaptic connections increases, the dispersion around zero decreases. This fact allows a cutoff in the expansions (9) and (12) in the case of uncorrelated patterns and sufficiently small values of α, yielding a reasonable comparison with biological systems, where higher-order multineuron effects are expected to be less frequent. In other words, it is reasonable to assume that binary synapses are the leading interactions and higher-order terms should become less important as the order increases and should be considered as correction terms. This is an important feature of the RS model and appears as an advantage of this model when compared to other multineuron interaction ones (see, for example, refs. 9 and 10). Although the number of k-order synapses increases as N^k as in other multineuron models, the fact that its dispersion around zero decreases means that the amount of information that can be allocated there decreases and the performance of the net is robust against defects in higher-order terms. Evidence for multineuron interactions in real systems are presented, for example, in ref. 18, where axon–axon synapses are described. This kind of coupling may change the strength of signals that are traveling through the axon coming from the cell body toward dendrite–axon connections: these are biological examples of multineuron interactions.

In particular, for the PAS case, when Eq. (12) is taken up to second order of synaptic connections, one gets

$$H \approx N\left(1 - \frac{1}{N^2} \sum_{i,j}^{N} \sum_{\mu=1}^{P} \xi_i^\mu \xi_j^\mu S_i S_j\right) \tag{16}$$

which is, up to constants, the expression for the energy function in the Hopfield model, Eqs. (6) and (7): in the limit of low load parameter α and uncorrelated patterns, one recovers the Hopfield Hamiltonian. When α increases or correlated patterns are considered, the Hopfield model yields unsatisfactory results,[4,7] the dispersion around zero of higher K orders increases, and more terms in expansion (12) should be taken into account. Here we are interested in analyzing the model given by Eq. (8). Truncation of the series will be studied elsewhere.

The expressions for the energy function in both the OPS and PAS cases can be rewritten in terms of the overlaps m_μ defined in Eq. (5). They are

$$H = N \prod_{\mu=1}^{N\alpha} (1 - m_\mu) \tag{17}$$

for the OPS network and

$$H = N \prod_{\mu=1}^{N\alpha} (1 - m_\mu^2) \tag{18}$$

for the PAS one. Here $P = N\alpha$ is the number of stored patterns. From these expressions one can study the extensivity of the model and deduce the critical load parameter for both cases. We first remark that a macroscopic overlap is only possible with a finite number of stored patterns. Consider, then, that the net is in such a state that it overlaps macroscopically with a finite number n of stored patterns and microscopically ($m \approx 1/\sqrt{N}$) with the remaining $P - n$ memories. The state of the net can then be described by the vector $\mathbf{m}$ that specifies the overlap of the net with every stored pattern:

$$\mathbf{m} = \left(m_1, m_2, \ldots, m_n, \pm \frac{1}{\sqrt{N}}, \ldots, \pm \frac{1}{\sqrt{N}} \right) \tag{19}$$

The energy per neuron for such a state is given by

$$\frac{E}{N} = (1 - m_1)(1 - m_2) \cdots (1 - m_n) \left(1 - \frac{1}{N} \right)^{(\alpha N - n)/2}$$

$$\xrightarrow{N \to \infty} (1 - m_1) \cdots (1 - m_n) \exp\left(-\frac{\alpha}{2} \right) \tag{20}$$

for the OPS case and by

$$\frac{E}{N} = (1 - m_1^2)(1 - m_2^2) \cdots (1 - m_n^2) \left(1 - \frac{1}{N} \right)^{(\alpha N - n)}$$

$$\xrightarrow{N \to \infty} (1 - m_1^2) \cdots (1 - m_n^2) \exp(-\alpha) \tag{21}$$

for the PAS configuration. The above equations show that the energy per neuron for an arbitrary state in both cases is finite and different from zero in the thermodynamic limit provided that $\alpha < \infty$. Also, in the case of the OPS configuration (when only the patterns are stored), it is useful to define a central state $\mathbf{C}$ in the direction of the sum vector of all stored patterns, which presents positive overlaps of the order of $1/\sqrt{P}$ with all memories. The energy per neuron of such a state is given by

$$E_{\mathrm{OPS}}[\mathbf{C}] = \left(1 - \frac{1}{(\alpha N)^{1/2}} \right)^{\alpha N} \xrightarrow{N \to \infty} \exp\left(-\frac{(\alpha N)^{1/2}}{2} \right) \tag{22}$$

The critical loading of the net is determined by the behavior of the energy per neuron in the thermodynamic limit ($N \to \infty$): as E/N is always zero for the stored patterns, the load limit at some temperature is determined by the lowering to zero of the energy barriers between them. For the PAS case this limit is attained only when $\alpha \to \infty$, i.e., the load capacity increases linearly with N, which is the superior limit behavior for any attractor neural network where the leading terms are related to binary synapses.[19] On the other hand, in the OPS configuration, when the number of stored patterns αN grows, the barriers between the patterns go to zero and $E[\mathbf{C}] \to 0$, but there still exists a big basin centered at the central state $\mathbf{C}$; the walls of this big basin, which have nonzero energies for finite α, are also lowered to zero only when $\alpha \to \infty$. The central state may be taken as the generalization of the taught patterns: it conserves the information common to all memories—the concept—and this generalization takes place for finite values of α. For zero activity and noncorrelated patterns in OPS nets, there is always only one central state (only one memorized concept); for other conveniently correlated sets of information many different central states may be found, both in PAS or OPS configurations. Up to now we have just presented some features of the RS model that can be inferred directly from the Hamiltonian (8) or its alternative forms.[12,13] The next section shows the mean-field calculations, performed using the same techniques as Amit *et al.*[4] for the Hopfield model.

3. MEAN-FIELD CALCULATIONS

We start by writing the partition function at finite temperature:

$$Z = \sum_{S_1, \ldots, S_N} \exp(-\beta H) \tag{23}$$

The temperature T, or its inverse β, is an external noise parameter. The sum over the spins S_i cannot be performed directly. Hence, we write

$$\sum_{S_1, \ldots, S_N} \exp(-\beta H) = \sum_{S_1, \ldots, S_N} \int_{-\infty}^{+\infty} dm_1 \cdots dm_P \times \left[\prod_{\mu=1}^{P} \delta\left(m_\mu - \frac{1}{N} \sum_{i=1}^{N} \xi_i^\mu S_i \right) \right] \exp[-\beta H(m_1, \ldots, m_P)] \tag{24}$$

where $H(m_1,..., m_P)$ is given by Eq. (17) or (18), depending on whether we are considering the OPS or the PAS case. We use the identity

$$\delta\left(m_\mu - \frac{1}{N}\sum_{i=1}^{N}\xi_i^\mu S_i\right) = \frac{\beta N}{2\pi \mathbf{i}}\int_{-i\infty}^{+i\infty} dt_\mu \times \exp\left[\beta N t_\mu\left(m_\mu - \frac{1}{N}\sum_{i=1}^{N}\xi_i^\mu S_i\right)\right] \tag{25}$$

in Eq. (24) and the sum over spins can now be performed. The partition function now reads

$$Z = \left(\frac{\beta N}{2\pi \mathbf{i}}\right)^P \int dm_1 \cdots dm_P \int dt_1 \cdots dt_P \exp[-\beta N f(\mathbf{m}, \mathbf{t})] \tag{26}$$

where $f(\mathbf{m}, \mathbf{t})$ is the free energy per neuron, defined as

$$f(\mathbf{m}, \mathbf{t}) = h(m_1,..., m_P) + \sum_{\mu=1}^{P} m_\mu t_\mu - \frac{1}{\beta N}\sum_{i=1}^{N} \ln\left[2\cosh\left(\beta \sum_{\mu=1}^{P}\xi_i^\mu t_\mu\right)\right] \tag{27}$$

with

$$h(m_1,..., m_P) = \prod_{\mu=1}^{P}(1 - m_\mu) \tag{28}$$

in the OPS case and

$$h(m_1,..., m_P) = \prod_{\mu=1}^{P}(1 - m_\mu^2) \tag{29}$$

for the PAS configuration.

As $f(\mathbf{m}, \mathbf{t})$ remains finite in the thermodynamic limit, the integrals in Eq. (26) may be solved through the saddle point method: the thermodynamic states described by the sets of values $\mathbf{m} = (m_1,..., m_P)$ and $\mathbf{t} = (t_1,..., t_P)$ that minimize $f(\mathbf{m}, \mathbf{t})$ are the equilibrium configurations of the net. Extremalizing Eq. (27), we obtain the following coupled equations for the overlaps:

$$m_\lambda = \frac{1}{N}\sum_{i=1}^{N}\xi_i^\lambda \tanh\left[\beta \sum_{\mu=1}^{P}\xi_i^\mu \prod_{\nu\neq\mu}^{P}(1 - m_\nu)\right] \tag{30}$$

in the OPS configuration and

$$m_\lambda = \frac{1}{N}\sum_{i=1}^{N}\xi_i^\lambda \tanh\left[2\beta \sum_{\mu=1}^{P}\xi_i^\mu m_\mu \prod_{\nu\neq\mu}^{P}(1 - m_\nu^2)\right] \tag{31}$$

for the PAS case, and the equations of state that relate **t** and **m** are

$$t_\mu = \prod_{\nu \neq \mu}^{P} (1 - m_\nu) \tag{32}$$

and

$$t_\mu = 2m_\mu \prod_{\nu \neq \mu}^{P} (1 - m_\nu^2) \tag{33}$$

for the OPS and PAS nets, respectively. Equations (30) and (31) are sets of P coupled transcendental equations whose solutions are not trivial. Up to now the averages implied by the sum over spins were not performed; they are necessary for the general solution at finite temperatures. Nevertheless, for zero temperature and the so-called proper memory solution, the model is exactly and easily soluble. Consider a state described by

$$\mathbf{m} = (1, m_{12}, m_{13}, \ldots, m_{1P}) \tag{34}$$

where $m_{1\nu} = (1/N) \sum_{i=1}^{N} \xi_i^1 \xi_i^\nu$ is the overlap between the memories ξ^1 and ξ^ν. Using Eq. (34) in (30) and (31), one obtains

$$m_\lambda = \frac{1}{N} \sum_{i=1}^{N} \xi_i^\lambda \tanh \left[\beta \xi_i^1 \prod_{\nu=2}^{P} (1 - m_\nu) \right] \xrightarrow{\beta \to \infty} m_{1\lambda} \tag{35}$$

in the OPS configuration and

$$m_\lambda = \frac{1}{N} \sum_{i=1}^{N} \xi_i^\lambda \tanh \left[2\beta \xi_i^1 \prod_{\nu=2}^{P} (1 - m_\nu^2) \right] \xrightarrow{\beta \to \infty} m_{1\lambda} \tag{36}$$

for the PAS configuration. This exact solution only reflects the fact that the memories are always minima of the energy. When finite temperatures are considered, the average value of the overlap m_1, for example, is no longer one and other terms besides the one in ξ^1 are present in the argument of the hyperbolic tangent: in this case we should average over the memories using the replica trick and/or self-average. Nevertheless, as the zero-temperature solutions are exact for all values of α and any set of stored patterns, the fluctuations responsible for phase transitions have a thermal origin. The limit in the load parameter for zero temperature is due to the lowering of the barriers to zero when $\alpha \to \infty$ and not to the dislocation of the minima of energy from the stored patterns to some spurious state, as happens to Hopfield-like models.

The qualitative difference between the behaviors for zero and finite values of α shown by Hopfield-like models arises from the dislocation of

the minima of energy, which requires more sophisticated averaging techniques such as the replica trick even at $T=0$. These different behaviors do not happen in our model, at least at $T=0$. In what follows we present separately the calculation for the PAS and OPS cases using the average over the memories as by Amit *et al.*[4]: for all values of α, at $T=0$ the results are exact. Calculations at finite temperatures within the replica trick approach are now in progress.

3.1. Patterns and Antipatterns—The PAS Case

We shall investigate solutions to Eqs. (31) that present an identical macroscopic overlap m with n memories (and implicitly $-m$ with the respective antimemories) and microscopic overlaps ($m \approx 1/\sqrt{N}$) with the other ones:

$$\mathbf{m} = (m, m, \ldots, m, 0, 0, \ldots, 0) \tag{37}$$

where we have omitted the overlaps with the antipatterns. Equation (31) now reads

$$m = \frac{1}{N} \sum_{i=1}^{N} \xi_i^{\mu} \tanh\left[2\beta m (1-m^2)^{n-1} \sum_{\lambda=1}^{n} \xi_i^{\lambda} \right]; \qquad \mu \leqslant n \tag{38}$$

and for $n < \mu \leqslant P$, Eq. (31) is always satisfied because the patterns are uncorrelated. Equation (38) can be solved by summing from $\mu = 1$ to n and reads

$$m = \frac{1}{Nn} \sum_{i=1}^{N} z_n^i \tanh[2\beta m (1-m^2)^{n-1} z_n^i] \tag{39}$$

where

$$z_n^i = \sum_{\mu=1}^{n} \xi_i^{\mu} \tag{40}$$

The site average can be rewritten as an average over z_n with the appropriate weights:

$$m = \frac{1}{2^n n} \sum_{k=0}^{n} \frac{n!}{k!\,(n-k)!} z_n \tanh[2\beta m (1-m^2)^{n-1} z_n] \tag{41}$$

with $z_n = n - 2k$.

The plot of the right-hand side (rhs) of Eq. (41) versus m is shown on Fig. 1 for different values of n and β. Clearly the paramagnetic state, $m=0$,

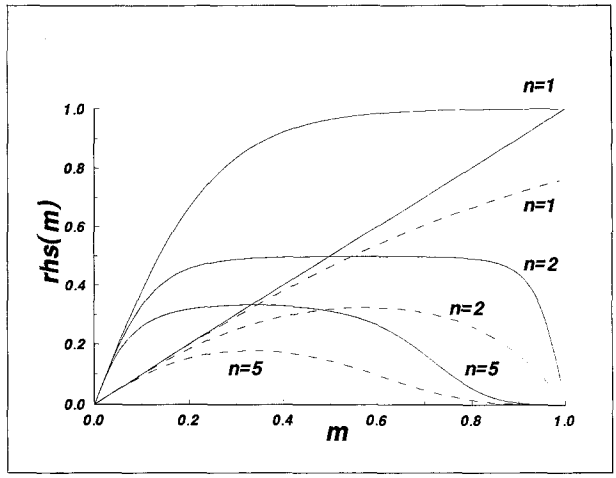

Fig. 1. Plot of the right-hand side of Eq. (41), rhs(m), for $n=1$, 2, and 5. The solid and dashed lines refer to $\beta=2$ and $\beta=0.5$, respectively. The straight line intercepts rhs(m) for $m>0$ only if $\beta>1/2$.

is always a solution of Eq. (41). The existence of $m\neq 0$ solutions is determined by the behavior of the rhs at $m\doteq 0$: they exist only if $\beta>1/2$; i.e., $T<2$. This critical temperature, $T_c=2$, is such that if $T>T_c$, the paramagnetic solution is the only stable configuration. For the Hopfield model, $T_c^{\mathrm{H}}=1$. The difference is due to the factor 1/2 that is absent in Eq. (16). The $m\neq 0$ solutions of Eq. (41) versus β for different values of n are shown on Fig. 2. The overlaps at the same temperature decrease with increasing n and go as $1/\sqrt{n}$ in the $T\to 0$ limit, for large n.

The stability of the solutions is determined by the behavior of $\delta^2 f$, calculated for the values of $\mathbf{m}$ that extremalize $f(\mathbf{m})$ [t is a function of $\mathbf{m}$, given by Eq. (33)]. One has

$$\delta^2 f = \sum_{\mu=1}^{n} [2(1-m^2)^{n-1} - 4\beta(1-m^2)^{2n-4} D_1]\, \delta m_\mu^2 + \sum_{\mu=n+1}^{P} [2(1-m^2)^n]\, \delta m_\mu^2 + \sum_{\mu=1}^{n} \sum_{\nu\neq\mu}^{n} [-4m^2(1-m^2)^{n-2} - 4\beta(1-m^2)^{2n-4} D_2]\, \delta m_\mu\, \delta m_\nu \quad (42)$$

where

$$D_1 = \frac{1}{nN} \sum_{i=1}^{N} \mathrm{sech}^2[2\beta m(1-m^2)^{n-1} z_n^i] \times \{(1+m^2)^2 n - 4m^2 (z_n^i)^2 [1-m^2(n-1)]\} \quad (43)$$

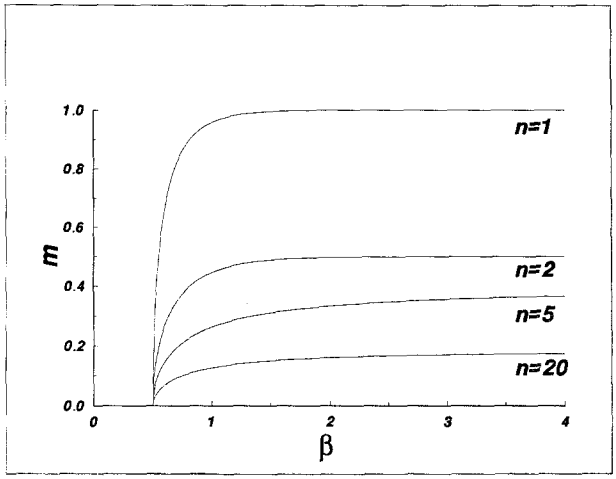

Fig. 2. The saddle point solutions m versus β for different values of n.

and

$$D_2 = \frac{1}{n(n-1)N} \sum_{i=1}^{N} \operatorname{sech}^2[2\beta m(1-m^2)^{n-1} z_n^i] \times \{(1+m^2)^2 [(z_n^i)^2 - n] - 4m^2(n-1)(z_n^i)^2 [1-m^2(n-1)]\} \quad (44)$$

Here, we have used the self-average property of the memories. The eigenvalues of the stability matrix $A_{\mu\nu} = \partial^2 f / \partial m_\mu \, \partial m_\nu$ are

$$\lambda_1 = 2(1-m^2)^n \quad (45)$$

which is $P-n$ times degenerate;

$$\lambda_2 = 2(1-m^2)^{n-2}(1+m^2) - 4\beta(1-m^2)^{2n-4}(D_1 - D_2) \quad (46)$$

which is $n-1$ times degenerate and does not exist if $n=1$; and finally,

$$\lambda_3 = 2(1-m^2)^{n-2}[1-(2n-1)m^2] - 4\beta(1-m^2)^{2n-4}[D_1 - (n-1)D_2] \quad (47)$$

which is nondegenerate.

For the paramagnetic solution, $m=0$, the eigenvalues are

$$\begin{aligned} \lambda_1 &= 2 \\ \lambda_2 &= 2 - 4\beta \\ \lambda_3 &= 2 - 4\beta \end{aligned} \quad (48)$$

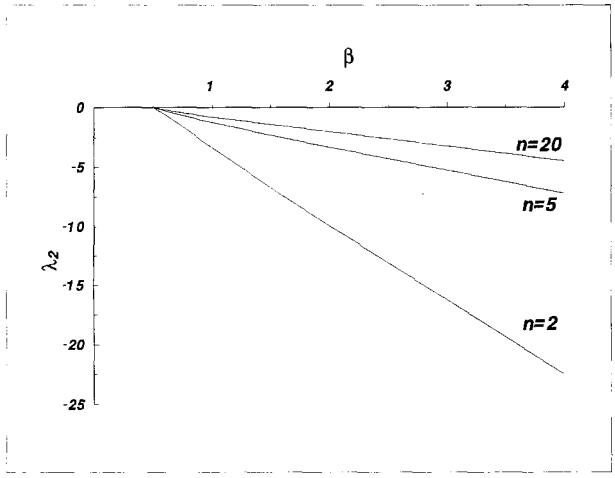

Fig. 3. Plot of λ_2 versus β for different values of $n > 1$. This eigenvalue is always negative in the region $\beta > 1/2$, where the solution $m \neq 0$ exists.

and they are nonnegative only if $\beta \leqslant 1/2$, i.e., the paramagnetic phase is stable only for $T \geqslant 2$.

When $n = 1$ and $m \neq 0$ there are only two different eigenvalues, λ_1 and λ_3, and both are nonnegative in the region $\beta \geqslant 1/2$, where the solution $m \neq 0$ holds: macroscopic overlaps with only one memory are stable solutions if $T < 2$. If $n \geqslant 2$, λ_2 is always negative for $\beta \geqslant 1/2$ and $m \neq 0$, going to zero as $\beta \to 1/2$, as one can see on Fig. 3, which shows the plot of λ_2 versus β for different values of n. These unstable solutions are states that overlap macroscopically with more than one pattern. One could have guessed this result from the form of the Hamiltonian, Eq. (8): equal overlaps with two patterns, for example, correspond to a point in the phase space halfway between two minima, which is surely a maximum in that direction. We have, then, the following scenario: for $T < 2$ the stable symmetric solution overlaps macroscopically with just one memory, and for $T \geqslant 2$ the paramagnetic state is the only stable solution. One could investigate other ansätze for asymmetric solutions, but both the form of the Hamiltonian, Eq. (8), and the results of numerical simulations[16,17] lead to the conclusion that they should not be stable.

3.2. Only Patterns—The OPS Case

To visualize the differences in the energy function between the PAS and the OPS situations, one must keep in mind that the antipatterns are located in a region in phase space that is the mirror image of the region

where the patterns are. When the antipatterns are also stored, these two regions present similar energy landscapes, but in the OPS case the antimemory region comprises very high-energy states and the phase space takes the form of an analogue of a multihole bowl in the closed space defined by the hypersurface of an N-dimensional hypercube. The greater is the number of patterns, the bigger is the difference between these two regions and the deeper is the bowl. The patterns are stored inside this big basin, whose center lies in the direction **C** determined by the sum of all stored uncorrelated patterns, as previously defined. As P increases, the size of the basins of attraction of each memory decreases, enlarging the probability that the network stabilizes in a state which is strongly correlated to the center of the big bowl. Figure 4 presents a pictorial sketch of the energy landscape of the phase space for this case. In the limit $P \to \infty$, the energy of the state in the center of the bowl goes to zero, the basins of attraction of each stored pattern merge, and there is only one big basin with a flat, zero-energy bottom in the region in phase space which is delimited by a ring obtained by linking the points associated to the patterns, centered at the direction **C**. Outside the ring the energy increases monotonically from zero to infinity, reaching its maximum value at the point $-\mathbf{C}$. This picture of the phase space agrees with results of numerical simulations,[16] where, for the OPS case, the relative size of the individual basins of attraction is determined by the absolute number P (for the PAS configuration they are

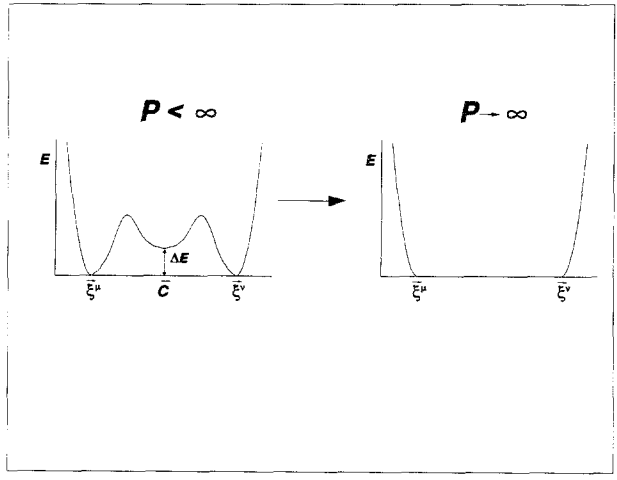

Fig. 4. Pictorial representation of the energy landscape in the phase space for the OPS case. For $P < \infty$ the direction **C**, determined by the sum of all stored patterns, is a local minimum of the Hamiltonian, with $E > 0$. In the $P \to \infty$ case the center of the big basin and all the stored patterns merge into a unique wide minimum.

determined by $\alpha = P/N$). The origin of the bowl comes from the first nontrivial term that appears in expansion (9):

$$h_1 = -\sum_i \left(\sum_{\mu=1}^{P} \xi_i^\mu \right) S_i \tag{49}$$

The central state **C** clearly minimizes that part of the Hamiltonian. This state has equal overlap with all the embedded patterns and is the center of the big bowl. In Fig. 5 we present the results of numerical simulations, where we measured the fraction of times that the net evolves to a pattern or to the central state **C** when starting from an initial overlap m_0 with the pattern.[16,17] The net should be set to a sufficiently similar initial state in order to retrieve a given pattern; otherwise it evolves toward the central state **C**.

In what follows we investigate the validity and stability of two different solutions to Eqs. (30), obtain the phase diagram for these ansätze, and interpret the results through the bowl-like shape of the phase space. Let us consider a solution of the kind

$$\mathbf{m} = (m, \varepsilon, \ldots, \varepsilon) \tag{50}$$

This solution reduces to the Mattis state ($\varepsilon = 0$) only at $T = 0$ due to the phase space anisotropy originated by the nonstoring of the antipatterns. In other words, for $T \neq 0$ the directions of the thermal fluctuations are not

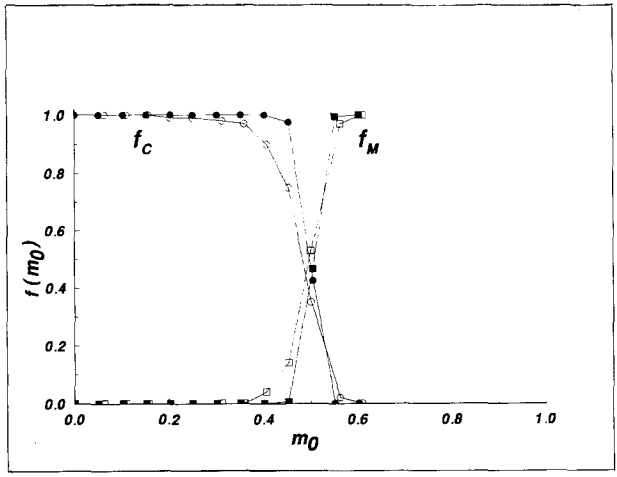

Fig. 5. Plot of numerical simulation results. The curve f_M is the fraction of times that the memory is recovered from an initial overlap m_0 and f_C is the fraction of times that the central state is recalled (see text), for network sizes of $N = 128$ (open symbols) and 512 (black symbols). The number of stored patterns is $P = 5$.

equiprobable, because the gradient is higher in the direction opposite to $\mathbf{C}$. Equation (30) now reads

$$\begin{aligned} m &= \frac{1}{N}\sum_{i=1}^{N} \xi_i^1 \tanh \beta \left[\xi_i^1 (1-\varepsilon)^{P-1} + \sum_{\mu=2}^{P} \xi_i^\mu (1-m)(1-\varepsilon)^{P-2} \right] \\ \varepsilon &= \frac{1}{N}\sum_{i=1}^{N} \xi_i^\nu \tanh \beta \left[\xi_i^1 (1-\varepsilon)^{P-1} + \sum_{\mu=2}^{P} \xi_i^\mu (1-m)(1-\varepsilon)^{P-2} \right], \qquad \nu \neq 1 \end{aligned} \tag{51}$$

Here, too, as in the preceding section, we consider uncorrelated patterns and substitute the average over sites i by averages over $z_{P-1}^i = \sum_{\mu=2}^{P} \xi_i^\mu$ and $z_1^i = \xi_i^1$, with the appropriate weights:

$$\begin{aligned} m &= \frac{1}{2^P} \sum_{l=0}^{1} \sum_{l'=0}^{P-1} \frac{(P-1)!}{l'!\,(P-1-l')!} (1-2l) \\ &\quad \times \tanh \beta [(1-2l)(1-\varepsilon)^{P-1} + (P-1-2l')(1-m)(1-\varepsilon)^{P-2}] \\ \varepsilon &= \frac{1}{P-1} \frac{1}{2^P} \sum_{l=0}^{1} \sum_{l'=0}^{P-1} \frac{(P-1)!}{l'!\,(P-1-l')!} (P-1-2l') \\ &\quad \times \tanh \beta [(1-2l)(1-\varepsilon)^{P-1} + (P-1-2l')(1-m)(1-\varepsilon)^{P-2}] \end{aligned} \tag{52}$$

where $1-2l = z_1$ and $P-1-2l' = z_{P-1}$.

The solutions to Eqs. (52) were obtained numerically. As one can see on Fig. 6, there are two branches for each value of P, one corresponding to the symmetric solution $m = \varepsilon$, which exists for every temperature, and

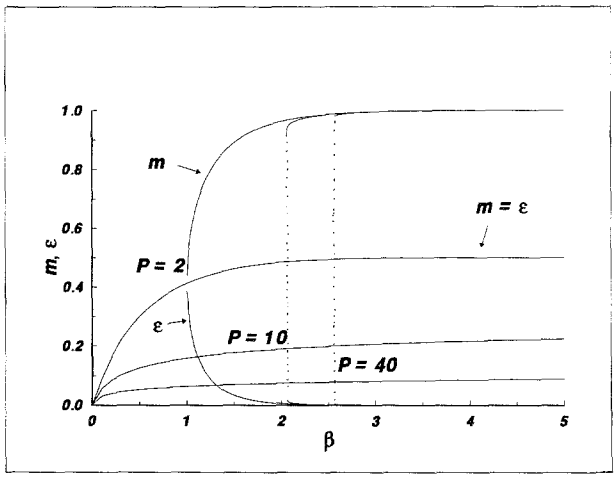

Fig. 6. The saddle point solutions m and ε of Eqs. (52) versus β for several values of P.

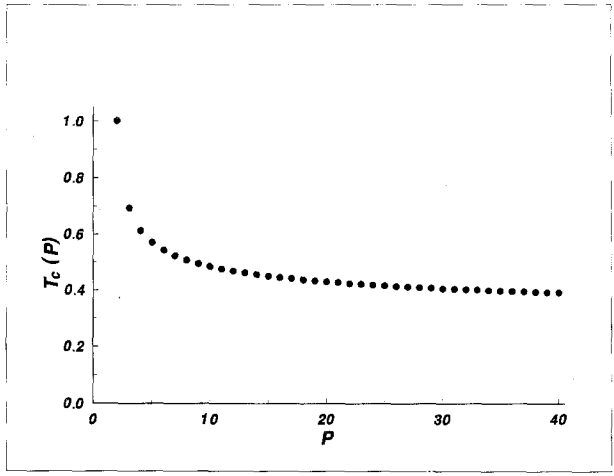

Fig. 7. The critical temperature $T_c(P)$ versus P at which the solution $m \neq \varepsilon$ ceases to exist. This temperature is a decreasing function of P.

another that is associated with the proper memory solution, $m \approx 1$ and $\varepsilon \approx 0$, and exists only for temperatures lower than a critical value T_c. On Fig. 7 one can see the plot of T_c as a function of P, in the $N \to \infty$ limit. When $P = 1$ this critical temperature goes to infinity: as the memorized pattern is the only minimum in energy, all the thermal fluctuations are isotropic around it and the average overlap with the pattern is always finite for finite temperatures. Also, the critical temperature $T_c(P)$ is a decreasing function of P because the greater the number of stored patterns, the easier it is to jump the energy barriers between the memories. On the other hand, when $T > T_c$, the only solution corresponds to a configuration that fluctuates thermally around the state $\mathbf{m} = (m, m, ..., m)$, which is the center of the bowl, in analogy to the $P = 1$ case, where the thermal fluctuations take place around the stored memory. At $T = 0$ this solution can be obtained analytically and reads

$$m = \frac{(P-1)!}{2^{P-1}[((P-1)/2)!]^2} \tag{53}$$

for odd P and

$$m = \frac{(P-1)!}{2^{P-1}(P/2)!\,(P/2-1)!} \tag{54}$$

for even P, and both forms (53) and (54) go as $1/\sqrt{P}$ as $P \to \infty$.

One must now investigate the stability of the solutions in their range of validity. We first calculate the stability matrix $A_{\mu\nu} = \partial^2 f / \partial m_\mu \, \partial m_\nu$, and obtain the eigenvalues. The matrix elements read

$$A_{\mu\nu} = -(1-\delta_{\mu\nu}) \prod_{\lambda \neq \mu,\nu}^{P} (1-m_\lambda) - \beta \sum_{\lambda \neq \mu}^{P} \sum_{\theta \neq \nu}^{P} T_{\lambda\theta} \left[\prod_{\kappa \neq \lambda,\mu}^{P} (1-m_\kappa) \right] \times \left[\prod_{\eta \neq \theta,\nu}^{P} (1-m_\eta) \right], \qquad \forall \mu \neq \nu \tag{55}$$

with

$$T_{\lambda\theta} = \frac{1}{N} \sum_{i=1}^{N} \xi_i^\lambda \xi_i^\theta \operatorname{sech}^2 \left[\beta \prod_{\kappa=1}^{P} \xi_i^\kappa \prod_{\eta \neq \kappa}^{P} (1-m_\eta) \right] \tag{56}$$

These matrix elements can be written, for the proper memory solution $\mathbf{m} = (m, \varepsilon, \ldots, \varepsilon)$, and considering the self-averaging of the patterns, as

$$A_{11} = -\frac{\beta(1-\varepsilon)^{P-1}}{2^P} \sum_{l=0}^{1} \sum_{l'=0}^{1} \sum_{l''=0}^{P-2} \frac{(P-2)!}{l''!\,(P-2-l'')!} \times [P-1-2(l'+l'')]^2 \operatorname{sech}^2(\Theta_1) \tag{57}$$

$$A_{1FD} = A_{1\mu} = A_{\mu 1} = \varepsilon - 1 - \frac{\beta(1-\varepsilon)^{P-2}}{2^P} \sum_{l=0}^{1} \sum_{l'=0}^{1} \sum_{l''=0}^{P-2} \frac{(P-2)!}{l''!\,(P-2-l'')!} \times [P-1-2(l'+l'')] \times [(1-\varepsilon)(1-2l) + (1-m)(P-2-2l'')] \operatorname{sech}^2(\Theta_1) \tag{58}$$

for $\mu \neq 1$,

$$A_D = A_{\mu\mu} = -\frac{\beta(1-\varepsilon)^{P-3}}{2^P} \sum_{l=0}^{1} \sum_{l'=0}^{1} \sum_{l''=0}^{P-2} \frac{(P-2)!}{l''!\,(P-2-l'')!} \times [(1-\varepsilon)(1-2l) + (1-m)(P-2-2l'')]^2 \operatorname{sech}^2(\Theta_1) \tag{59}$$

again for $\mu \neq 1$, and finally,

$$A_{FD} = A_{\mu\nu}$$
$$= m - 1 - \frac{\beta(1-\varepsilon)^{P-3}}{2^P} \sum_{l=0}^{1} \sum_{l'=0}^{1} \sum_{l''=0}^{1} \sum_{l'''=0}^{P-3} \frac{(P-3)!}{l'''!\,(P-3-l''')!}$$
$$\times \{(1-\varepsilon)^2 + (1-m)[P-2-2(l'+l''')]$$
$$\times [2(1-\varepsilon)(1-2l) + (1-m)(P-2-2(l''+l'''))]\} \operatorname{sech}^2(\Theta_2) \tag{60}$$

for $\mu, \nu \neq 1$, $\mu \neq \nu$. The functions Θ_1 and Θ_2 are defined as

$$\Theta_1 = \beta(1-\varepsilon)^{P-2}$$
$$\times [(1-2l)(1-\varepsilon) + (1-2l')(1-m) + (P-2-2l'')(1-m)] \tag{61}$$
$$\Theta_2 = \beta(1-\varepsilon)^{P-2}$$
$$\times \{(1-2l)(1-\varepsilon) + (1-2l')(1-m)$$
$$+ (1-m)[P-2-2(l''+l''')]\} \tag{62}$$

A matrix with such a structure has the following eigenvalues:

$$\lambda_1 = A_D - A_{FD} \tag{63}$$
$$\lambda_2 = \tfrac{1}{2}[A_{11} + A_D + (P-2)\,A_{FD}]$$
$$+ \tfrac{1}{2}\{[A_{11} - A_D - (P-2)\,A_{FD}]^2 + 4(P-1)\,A_{1FD}^2\}^{1/2} \tag{64}$$
$$\lambda_3 = \tfrac{1}{2}[A_{11} + A_D + (P-2)\,A_{FD}]$$
$$- \tfrac{1}{2}\{[A_{11} - A_D - (P-2)\,A_{FD}]^2 + 4(P-1)\,A_{1FD}^2\}^{1/2} \tag{65}$$

The eigenvalue λ_1 is $(P-2)$ times degenerate, while λ_2 and λ_3 are non-degenerate. On Fig. 8 we plot these eigenvalues versus β, for a fixed $P=5$; the behavior is analogous for every $P>1$. The critical temperature at which λ_2 goes to zero is the same at which the proper memory solution no longer exists, $T_c(P)$. Consequently, in the range of validity of this solution, there is no change of sign in any of the eigenvalues of the stability matrix. At $T=0$ $(\beta \to \infty)$ the proper memory solution is clearly stable; then we conclude that the proper memory solution, when it exists, is always stable.

To study the stability of the symmetric solution $\mathbf{m} = (m, m, \ldots, m)$, it is sufficient to replace ε by m in Eqs. (57)–(62). In this case, $A_{11} = A_D$ and $A_{1FD} = A_{FD}$ and the eigenvalues read

$$\lambda_1' = 1 - \frac{\beta(1-m)^{P-2}}{P-1} \frac{1}{2^P} \sum_{l=0}^{P} \frac{P!}{l!\,(P-l)!} \left[P - \frac{1}{P}(P-2l)^2\right]$$
$$\times \operatorname{sech}^2[\beta(1-m)^{P-1}(P-2l)] \tag{66}$$

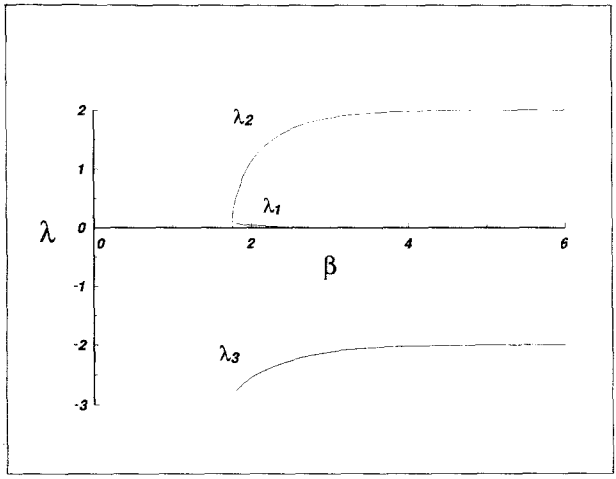

Fig. 8. Plot of the eigenvalues of the stability matrix versus β for the $m \neq \varepsilon$ solution and $P = 5$. Here λ_1 is always positive, λ_3 is always negative, and λ_2 goes to zero as T goes to $T_c(P)$. This behavior is analogous for every value of P.

which is $P-1$ times degenerate and

$$\lambda_2' = 1 - P - \beta(1-m)^{P-2} \frac{1}{2^P} \sum_{l=0}^{P} \frac{P!}{l!\,(P-l)!} (P-2l)^2 \left(P - 2 + \frac{1}{P}\right) \times \operatorname{sech}^2[\beta(1-m)^{P-1}(P-2l)] \tag{67}$$

which is nondegenerate.

The eigenvalue λ_2' is always negative for every value of temperature. On the other hand, λ_1' may change sign, depending on whether P is odd or even, as one can see on Fig. 9. In the limit $T \to \infty$, this solution is clearly stable; consequently, for odd P, the symmetric solution $\mathbf{m} = (m, m, \ldots, m)$ is always stable, while for even P, it may become unstable as $T \to 0$ at a temperature T_c^S given by the change of signal of λ_1', which can be obtained from Eq. (66):

$$T_c^S \cong \frac{P^2(P-2)!\,(1-m)^{P-2}}{2^P[(P/2)!]^2} \tag{68}$$

where m can be replaced by its $T \to 0$ limit [Eq. (54)]. On Fig. 10 the phase diagram for the OPS nets has been represented in the plane T versus P: in region III just the symmetric overlap solution (disordered state) is stable. In region II both symmetric and proper memory solutions are stable, and in region I, the proper memory is stable and the symmetric

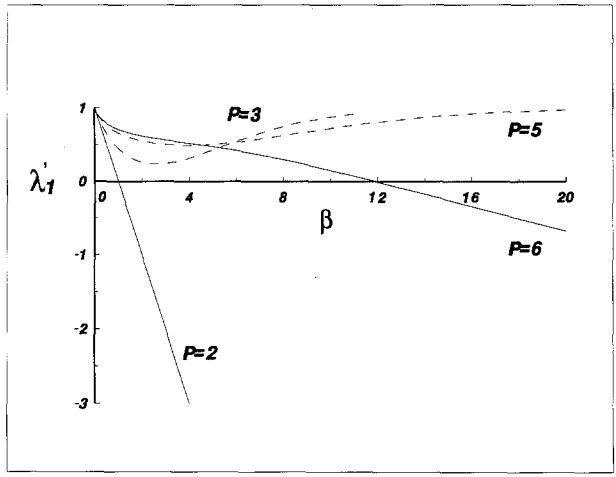

Fig. 9. Plot of λ_1' versus β for different values of P. This eigenvalue is always positive if P is odd and changes sign at T_c^S for even P.

solution is unstable only for even values of P. Equation (68) defines the border between regions I and II. The difference between odd and even P is observable only if P is very low ($\leqslant 10$). On the other hand, as $P \to \infty$ such that $\alpha = P/N$ remains finite, all basins of attraction of stored patterns merge and the only stable phase is III ($T_c \to 0$ as $P \to \infty$): the configuration of the

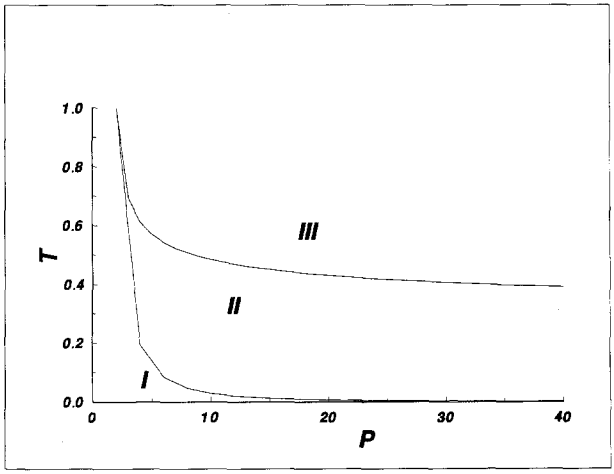

Fig. 10. Phase diagram for the OPS net. In region III just the symmetric solution ($m = \varepsilon$) is stable; in region II both symmetric and proper ($m \neq \varepsilon$) solutions are stable; and in region I, the proper memory is stable and the symmetric solution is unstable only for even P.

net fluctuates isotropically around the center of the bowl. This behavior is also observed in numerical simulations,[16] where we found that the sizes of the individual basins of attraction go to zero as P increases, regardless of the size of the net N.

4. DISCUSSION AND CONCLUSIONS

The RS model has been presented in full detail and the phase diagram has been obtained in mean field. Two extreme situations were considered: PAS (patterns and antipatterns) and OPS (only patterns) configurations. In both cases the energy function of the net is nonnegative and the patterns always present zero energy. As a consequence, the memories are always minima of energy regardless of the load parameter α and for any set of stored patterns. The limit in the load parameter then has the following origin: the minima remain at the stored patterns, but the heights of the energy barriers are lowered to zero as α goes to infinity. An exact proper memory solution is then possible at $T=0$ for finite values of α and any set of stored patterns.

In particular, the PAS configuration presents a very simple phase diagram: if $T<T_c=2$, only proper memory solutions are stable, while if $T>T_c=2$, only the paramagnetic solutions are stable. When more sophisticated averaging processes are utilized, one expects the net to present a qualitatively similar behavior except for the transition temperature, which will be renormalized as α increases such that $T_c \to 0$ as $\alpha \to \infty$.

Also, the PAS configuration recovers the Hopfield model in the limit of uncorrelated patterns and low load parameter, when multineuron interaction terms may be neglected in the energy function. However, as α increases and/or correlations between the memories are considered, these terms are no longer negligible and must be taken into account. Here we have calculated the properties of the solutions of the full model. A study of a "truncated model" where only corrections of low-order couplings (4, 6) are considered—more adequate to the description of biological systems—is now in progress and preliminary results shows that these low-order terms are enough to significantly improve the performance of the net as an associative memory device.

On the other hand, the OPS configuration presents interesting features because of the anisotropic energy landscape in phase space with a big basin of attraction in the phase space, centered at the state **C**, defined by the direction of the vector sum of all stored patterns. The stored patterns also present smaller individual basins of attraction inside of the big basin, like holes in a bowl. The walls of the big bowl are lowered to zero when α goes

to infinity, but before that, when the number P of stored patterns increases, regardless of the size of the net N the individual basins of attraction merge, the big basin presents a flat, zero-energy bottom, and the only stable state is the central state **C**. This can be interpreted as a generalization of the learnt patterns: it conserves only the information that is common to all memories. Of course, in the case of uncorrelated patterns there is only one central state, that is, only one memorized concept. For conveniently correlated patterns, for both OPS and PAS configurations, many central states may coexist: many concepts which are uncorrelated among themselves may be learnt by the net from adequately chosen examples. The behavior of the net around these central states is expected to follow qualitatively the OPS, uncorrelated memory configuration.

In summary, the RS model provides a prescription for an associative memory that has the following properties: (i) considers multineuron interaction effects, preserving the binary interaction, (ii) presents, for finite α, zero-temperature exact proper memory solutions, (iii) does not exhibit the "minima dislocation effect" when increasing the load of the net, and (iv) seems to yield a direct route to model associative memories that are able to learn and generalize from examples.

ACKNOWLEDGMENTS

We acknowledge fruitful discussions with Drs. T. J. P. Penna and P. M. C. de Oliveira. This work was partially supported by Brazilian agencies Conselho Nacional de Desenvolvimento Científico e Tecnológico (CNPq), Financiadora de Estudos e Projetos (FINEP), and Fundação de Amparo à Pesquisa do Estado do Rio Grande do Sul (FAPERGS).

REFERENCES

1. W. S. McCulloch and W. A. Pitts, *Bull. Math. Biophys.* **5**:115 (1943).
2. J. J. Hopfield, *Proc. Natl. Acad. Sci. USA* **79**:2554 (1982).
3. D. J. Amit, *Modeling Brain Function* (Cambridge University Press, Cambridge, 1989).
4. D. J. Amit, H. Gutfreund, and H. Sompolinsky, *Phys. Rev. A* **32**:1007 (1985); *Ann. Phys.* (N.Y.) **173**:30 (1987); *Phys. Rev. A* **35**:2293 (1987).
5. E. Gardner, *J. Phys. A: Math. Gen.* **21**:257 (1988).
6. D. O. Hebb, *The Organisation of Behavior* (Wiley, New York, 1949).
7. T. J. P. Penna and P. M. C. Oliveira, *Europhys. Lett.* **11**(3):191 (1990).
8. L. Personnaz, I. Guyon and G. Dreyfus, *J. Phys. Lett.* (Paris) **46**:L359 (1985).
9. I. Kanter and H. Sompolinsky, *Phys. Rev. A* **35**:380 (1987).
10. E. Gardner, *J. Phys. A: Math. Gen.* **20**:3453 (1987).
11. G. A. Kohring, *J. Phys.* (Paris) **51**:145 (1990).
12. R. M. C. de Almeida and J. R. Iglesias, *Phys. Lett. A* **146**:239 (1990).

13. J. J. Arenzon, R. M. C. de Almeida, and J. R. Iglesias, in: *Nonlinear Phenomena in Fluids, Solids and other Complex Systems*, P. Cordero and B. Nachtergaele, eds. (North-Holland, Amsterdam, 1991), p. 21.
14. D. Horn and M. Usher, *J. Phys.* (Paris) **49**:389 (1988).
15. L. F. Abbott and Y. Arian, *Phys. Rev. A* **36**:5091 (1987).
16. J. J. Arenzon, R. M. C. de Almeida, J. R. Iglesias, T. J. P. Penna, and P. M. C. de Oliveira, *J. Phys. I* (Paris) **1**:55 (1992).
17. T. J. P. Penna, P. M. C. de Oliveira, J. J. Arenzon, R. M. C. de Almeida, and J. R. Iglesias, *Int. J. Mod. Phys. C* **2**:711 (1991).
18. P. Peretto and J. J. Niez, *Biol. Cybernet.* **54**:53 (1986).
19. V. Deshpande and C. Dasgupta, *J. Stat. Phys.* **64**:755 (1991).